

Spin-conserving and reversing photoemission from the surface states of Bi₂Se₃ and Au (111)

Ji Hoon Ryoo and Cheol-Hwan Park*

Department of Physics, Seoul National University, Seoul 08826, Korea

(Dated: March 1, 2016)

We present a theory based on first-principles calculations explaining (i) why the tunability of spin polarizations of photoelectrons from Bi₂Se₃ (111) depends on the band index and Bloch wavevector of the surface state and (ii) why such tunability is absent in the case of *isosymmetric* Au (111). The results provide not only an explanation for the recent, puzzling experimental observations but also a guide toward making highly-tunable spin-polarized electron sources from topological insulators.

Since the beginning of spintronics, constant efforts have been made to generate electrons with a high degree of spin polarization using transport [1], optical [2], and magnetic resonance methods [3]. In particular, optical methods, also known as optical spin orientation, use polarized-light irradiation. For example, electrons in the valence band of strained and surface-treated GaAs can be excited by circularly polarized light and emitted with $\sim 80\%$ spin polarization [4]. GaAs photocathodes are widely used as spin-polarized electron source in low-energy electron microscopy [5], in accelerators used in high-energy physics [6], etc.

Recently, it has been proposed that topological insulators can serve as a spin-polarized electron source when irradiated with polarized light [7]. By changing the polarization of light and the direction toward which photoelectrons are collected, one can obtain an electron beam which is spin-polarized in an arbitrary direction, with a 100 % degree of spin polarization [8] (the measured degree is over 80 % [9]). On the other hand, the direction of spin polarization of electrons generated from a strained-GaAs photocathode is fixed by the surface-normal direction perpendicular to which the strain is applied. Moreover, unlike GaAs photocathodes, in which the photon energy is fixed to ~ 1.5 eV by the material band gap, photocathodes using a topological insulator can be operated within a wide range of photon energies. Even if there could be several technological hurdles that should be overcome, topological insulators are conceptually new candidates for photocathodes for spintronics.

Despite these recent developments, we still do not understand the results from some of the key spin- and angle-resolved photoemission spectroscopy (SARPES) experiments on the surface of the Bi₂Se₃ family of topological insulators, whose space group is $R\bar{3}m$, such as Bi₂Se₃, Bi₂Te₃ and Sb₂Te₃. Jozwiak *et al.* [7] studied photoelectrons ejected from the Dirac-cone-like surface band of Bi₂Se₃ and the Rashba-split surface band of Au (Fig. 1). When shone on a Bi₂Se₃ (111) surface, p-polarized light generates photoelectrons whose spin direction is parallel to that of the surface electrons, while s-polarized light produces photoelectrons with the opposite spin [7]. Since the Bi₂Se₃ and Au (111) surfaces have the same symme-

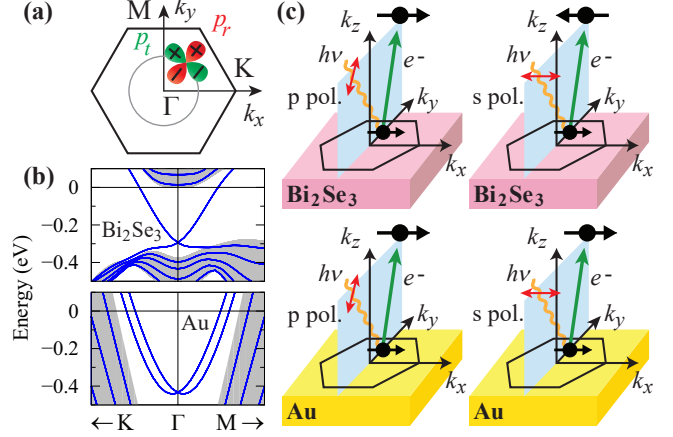


FIG. 1. (a) The Brillouin zone of Bi₂Se₃ and Au surfaces. The p_r and p_t orbitals of a given Bloch state specified by the Bloch wavevector $\mathbf{k} = k(\cos\phi_k, \sin\phi_k)$ are defined as $p_r = \cos\phi_k p_x + \sin\phi_k p_y$ and $p_t = -\sin\phi_k p_x + \cos\phi_k p_y$, respectively, where p_x and p_y are the valence atomic p orbitals. (b) The bandstructures (blue curves) of the (111) surfaces of Bi₂Se₃ and Au along $(0.14, 0) \rightarrow (0, 0) \rightarrow (0, 0.14)$ in reciprocal space in units of $2\pi/a$, where a is the lattice parameter. Projected bulk bands are also shown in gray. (c) Schematics of the SARPES experimental setup and the results of Ref. [7]. The horizontal arrows denote the direction of the spin polarization of the surface electrons and photoelectrons.

try, the theoretical analysis predicts that the gold surface would also exhibit the same photo-induced spin modulation as Bi₂Se₃ (111) [8]. The SARPES experiment for the gold surface [7] clearly resolves the two spin-split bands; however, both s- and p-polarized lights produce photoelectrons with the same spin direction as that of the initial state in each surface band [Fig. 1(c)].

Also, another experimental study on Bi₂Se₃ (111) has shown that photoemission from the upper branch of the surface bands exhibits such photo-induced spin modulation, while that from the lower branch does not [10]. In an effort to explain this observation, it was claimed that s-polarized light probes the spinor that couples to p_r orbital, because the electronic states in the lower branch have more p_r character than p_t one [11] [for the definition of p_r and p_t orbitals, see Fig. 1(a)]. However, the spinor

being measured is the one coupled to the orbital interacting with s-polarized light (p_t), and not the one coupled to the dominant p orbital (p_r). Therefore, the experimental observation cannot be understood from previous theories [8, 11].

In summary, we still do not have a good understanding of the photo-induced spin modulation phenomenon involving the Bi_2Se_3 family of topological insulators. In this study, we perform first-principles calculations on the spin polarization of photoelectrons ejected from the Bi_2Se_3 and Au (111) surfaces. First of all, our results agree with the recent experimental observations in Refs. [7, 10] that were not understood before. We show that the complicated, material-dependent coupling between the spinor part and the orbital part of the wavefunctions plays a central role in determining the spin polarization from these surfaces. We also show that this spinor-orbital coupling in the wavefunction of Bi_2Se_3 , in particular, depends heavily on both the direction and magnitude of the Bloch wavevector; the pronounced deviation of the spinor-orbital coupling from the one near the Dirac point is seen in the lower branch along ΓK , where the low-energy effective theories [8, 11] predict that the direction of the spin polarization of photoelectrons is the opposite of the experimental observation [10]. Our results provide a theoretical background for developing next-generation spin-polarized electron sources.

To obtain the spin polarization of photoelectrons, we calculate the matrix elements of $\mathbf{A} \cdot \mathbf{p}$, where \mathbf{A} is a vector parallel to the polarization of light and \mathbf{p} the momentum operator, between the initial surface state and the two (spin-up and spin-down) photoexcited states. This method of using the dipole transition operator to account for light-matter interactions reproduces the measured spin polarization of photoelectrons ejected from Bi_2Se_3 quite successfully [12, 13]. For computational details, see Supplemental Material [14]. To simulate low-energy photoemission experiments [7, 10], we set the photon energy to 6 eV.

We denote the incoming direction of incident photons by $(-\sin\theta_{\text{ph}}\cos\phi_{\text{ph}}, -\sin\theta_{\text{ph}}\sin\phi_{\text{ph}}, -\cos\theta_{\text{ph}})$ and the outgoing direction of photoelectrons by $(\sin\theta_e\cos\phi_e, \sin\theta_e\sin\phi_e, \cos\theta_e)$. We focus mainly on two cases: $\phi_{\text{ph}} = \pm 90^\circ$ and $\phi_e = \pm 90^\circ$ (i.e., the in-plane momenta of light and photoelectrons are along ΓM) and $\phi_{\text{ph}} = 0^\circ$ or 180° and $\phi_e = 0^\circ$ or 180° (along ΓK).

First, we compare the spin polarization of photoelectrons emitted from the upper band of the surface states of Bi_2Se_3 (111) [Fig. 1(c)] and of Au (111) [Fig. 1(d)] when the incident photons and photoelectrons both lie in the mirror plane, which is perpendicular to ΓK ($\phi_{\text{ph}} = \pm 90^\circ$ and $\phi_e = 90^\circ$). [For $\phi_e = -90^\circ$, similar results are obtained provided the sign of ϕ_{ph} is flipped in Fig. 2 (not shown)]. We define the spin polarization vector (without $\hbar/2$) \mathbf{P} of a certain state as the expectation value of the Pauli spin operators taken for that state. Then, due

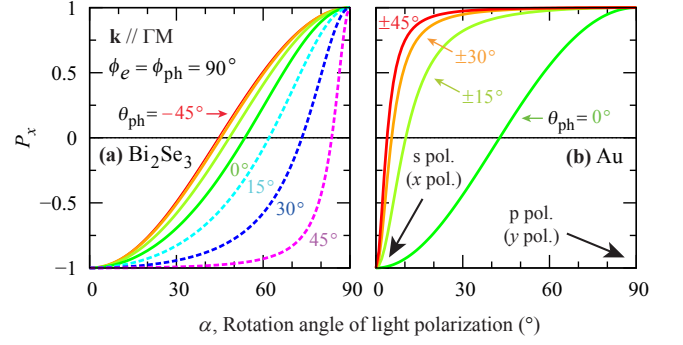


FIG. 2. The spin polarization along x , P_x , of photoelectrons emitted from Bi_2Se_3 (111) [(a)] and from Au (111) [(b)]. Note that, for notational convenience, we have used negative θ_{ph} to denote cases with $\phi_{\text{ph}} = -90^\circ$. The initial surface state is in the upper band and has $\mathbf{k} = 0.01 (2\pi/a) \hat{y}$.

to the mirror symmetry, (i) \mathbf{P} of any surface state with Bloch wavevector \mathbf{k} along ΓM is parallel or antiparallel to ΓK and (ii) the p- and s-polarized photons generate photoelectrons characterized by \mathbf{P} which is 100 % in magnitude and is, respectively, parallel to and antiparallel to the \mathbf{P} of the surface state [8]. This symmetry analysis is in agreement with the SARPES experimental results on Bi_2Se_3 (111) [7, 13, 15].

Since Bi_2Se_3 (111) and Au (111) have the same symmetry, one would naturally expect that the same symmetry analysis holds for Au (111); however, it was observed that photoelectrons from the gold surface have the same spin polarization independent of the direction of \mathbf{A} [7].

In order to understand these seemingly contradictory results for Au (111), we calculate P_x of photoelectrons as a function of the rotation angle α of light polarization (Fig. 2). For s- and p-polarized light (α being 0° and 90° , respectively) the calculated P_x for both Bi_2Se_3 (111) and Au (111) is in accord with the symmetry-based theoretical prediction. A first-principles study also reported the spin reversal of photoelectrons ejected from Au (111) by s-polarized light and the spin conservation by p-polarized light [16]. However, the Bi_2Se_3 and Au surfaces exhibit differences in the manner P_x changes in between (Fig. 2).

We first consider the case $\theta_{\text{ph}} = 45^\circ$ (corresponding to the curves in Fig. 2 with $\theta_{\text{ph}} = \pm 45^\circ$). For Bi_2Se_3 , P_x -versus- α relations for $\phi_{\text{ph}} = 90^\circ$ and for $\phi_{\text{ph}} = -90^\circ$ (denoted by negative θ_{ph} in Fig. 2) are qualitatively different [Fig. 2 (a)]: (i) when $\phi_{\text{ph}} = -90^\circ$, P_x varies slowly with α from -1 to 1 , changing the sign near $\alpha = 45^\circ$; (ii) when $\phi_{\text{ph}} = 90^\circ$, P_x remains negative as long as $\alpha < 83^\circ$. On the other hand, for Au, the dependence of P_x on α for $\phi_{\text{ph}} = 90^\circ$ and that for $\phi_{\text{ph}} = -90^\circ$ are essentially the same. In both cases, P_x changes sharply from -1 to nearly 1 at small α [$P_x = 0$ at $\alpha = 3^\circ$; see Fig. 2(b)].

This difference between the two materials on how P_x changes with α originates from the difference in the

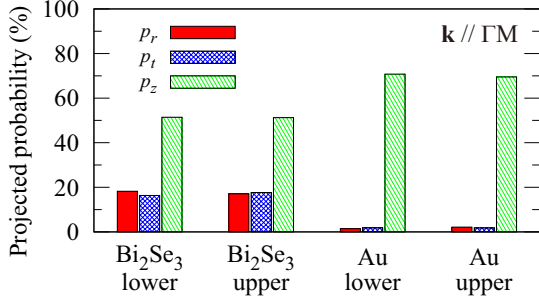


FIG. 3. The projected probability (i.e., squared amplitude) to each p orbital of the surface state with $\mathbf{k} = 0.01 (2\pi/a) \hat{y}$.

surface-state wavefunctions. Among the orbitals constituting the (initial) surface states, we focus on p orbitals which play a dominant role in photoemission when the final states have s -like characters. This scheme successfully describes the results from low-energy SARPES experiments on Bi₂Se₃ [13, 17].

Figure 3 shows squared projections of the surface states near Γ of Bi₂Se₃ and Au to each valence p orbital, summed over atomic sites. In Bi₂Se₃ case, the contribution of in-plane p -orbitals (p_r and p_t) to the surface states is 35%, similar in magnitude to that of p_z orbital (51%). On the contrary, each in-plane orbital (p_r or p_t) of Au contributes less than 2% to the surface state of Au (111). The results on Au (111) are consistent with previous studies [18, 19].

Although the symmetry analysis indicates that each p orbital comprising the gold surface states couples to spinors in the same way as in the case of Bi₂Se₃, since the surface states of Au has almost no in-plane p -orbital character, the spin degree of freedom is *not* entangled with the orbital ones. Therefore, if A_z is finite, even if it is small, \mathbf{P} of photoelectrons from the gold surface is almost completely determined by the spinor coupled to the p_z orbital of the surface state. Thus, P_x rises sharply as α deviates from 0° [Fig. 2(b)].

We compare P_x 's of photoelectrons associated with $\phi_{\text{ph}} = 90^\circ$ and that associated with $\phi_{\text{ph}} = -90^\circ$. The light polarization vectors for these two cases are the same except that the signs of their out-of-plane components are opposite. Because the spinors attached to in-plane and out-of-plane p orbitals interfere with each other differently in the two cases, the corresponding \mathbf{P} 's are in principle different. This effect is sizable for Bi₂Se₃ (111) [Fig. 2(a)] but is negligible for Au (111) [Fig. 2(b)] because, again, the contribution of in-plane p orbitals to the surface states of Au (111) is small.

The dependence of P_x on θ_{ph} (Fig. 2) further illustrates the importance of the entanglement between the spin and orbital degrees of freedom in photoemission processes. When $\theta_{\text{ph}} = 0^\circ$ (i.e., normal incidence), $A_z = 0$,

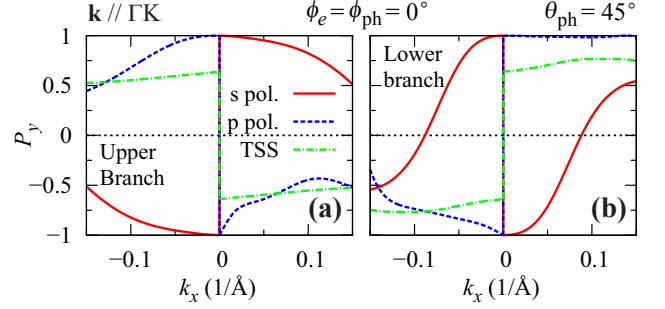


FIG. 4. The spin polarization of photoelectrons along y , P_y , emitted from Bi₂Se₃ (111) surface states with \mathbf{k} along ΓK . The dash-dotted or green curve shows P_y of the initial topological surface state (TSS).

and only the in-plane p orbitals are probed. Therefore, in this case, P_x of photoelectrons from both Bi₂Se₃ and Au surfaces changes slowly with α from -1 to 1 . When θ_{ph} increases from 0° to 15° , A_z becomes finite; therefore, the dependence of P_x of photoelectrons from Au (111) on α significantly changes, becoming similar to that corresponding to $\theta_{\text{ph}} = 45^\circ$. For Bi₂Se₃, however, this increase in θ_{ph} does not have such a huge effect on P_x .

From the results of our calculations, we can understand the hitherto incomprehensible differences in the results of SARPES experiments on Bi₂Se₃ and Au surfaces [7]. If the light with *perfect* s -polarization excites a surface state, the measured \mathbf{P} must be antiparallel to the spin polarization of the surface state for both Bi₂Se₃ and Au. In real experiments, however, the “ s -polarized” light may contain a few percent of the p component due to the imperfection of the polarizer, the inaccuracy in the alignment, or the inhomogeneity of the surface. Our calculations [Fig. 2(b)] suggest that this small fraction of p -polarized light may determine the spin polarization of photoelectrons from Au (111), which explains the experimental result [7] that s - and p -polarized lights produce photoelectrons with similar \mathbf{P} 's and that photo-induced spin modulation is hard to achieve with Au (111).

We now discuss the SARPES configuration $\phi_{\text{ph}} = 0^\circ$ and $\phi_e = 0^\circ$, i.e., photons and electrons have the in-plane momenta parallel to ΓK . In this case, no symmetry principle restricts the spin direction of surface electrons or photoelectrons. Nevertheless, when \mathbf{k} of a surface state is small, according to first-order $\mathbf{k} \cdot \mathbf{p}$ perturbation theory [11], the p_r and p_z orbitals in the surface states always couple to the spinor $|\downarrow_t\rangle$ and the p_t orbital to $|\uparrow_t\rangle$ in the upper branch, where $|\uparrow_t\rangle$ and $|\downarrow_t\rangle$ are the eigenspinors of $\sigma_t = \boldsymbol{\sigma} \cdot (\hat{z} \times \hat{k})$ with eigenvalues 1 and -1 , respectively. (The three p orbitals couple to the opposite spinors in the lower branch.) Therefore, for a small k , \mathbf{P} of the photoelectrons generated by p - and s -polarized lights are parallel to and antiparallel to the \mathbf{P} of the surface state, respectively.

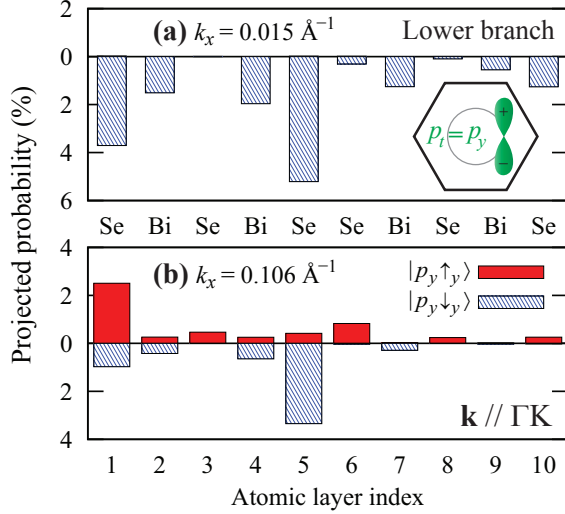


FIG. 5. Projected probability to the p_t orbital in each atomic layer of the surface states in the lower branch at $\mathbf{k} = 0.015 \text{ \AA}^{-1} \hat{x}$ [(a)] and at $\mathbf{k} = 0.106 \text{ \AA}^{-1} \hat{x}$ [(b)]. The spin is quantized along y . Atomic layer 1 is the topmost surface layer.

However, first-order $\mathbf{k} \cdot \mathbf{p}$ theory is valid only at a small k : the couplings between orbitals and spinors that are forbidden near Γ (e.g., p_r and $|\downarrow_t\rangle$ or p_t and $|\uparrow_t\rangle$ in the lower branch) are allowed if second or higher order effects are considered. These couplings are anisotropic in that if \mathbf{k} is along ΓM they are strictly forbidden even at a large k . For Au (111), these higher-order spin-orbital entanglement effects are difficult to observe due to the dominance of p_z character in the surface state; however, for Bi_2Se_3 (111), in the lower branch along ΓK , they significantly affect the photoemission process if k is not small (Fig. 4).

Figure 4 shows that, when probing the lower branch with large k_x , s-polarized light as well as p-polarized light yields photoelectrons whose P_y (the tangential component of \mathbf{P}) has the same sign as P_y of the surface state, contrary to the small- k results. In the case of the upper branch, this stark sign change of the spin polarization is not observed in our calculation. The results at large k are confirmed by recent experiments [10].

It was suggested that this lack of photo-induced spin modulation associated with the surface state in the lower branch was due to the dominance of p_r orbital in the corresponding surface state which couples to $|\uparrow_t\rangle$ [10]. However, since s-polarized light picks up the spinor coupled to p_t orbital and not the spinor coupled to the dominant p orbital (i.e., p_r), this explanation is not satisfactory. Instead, we show in the following that the origin of this phenomenon is the complex spin-orbital coupling in the initial surface state at large k , which is absent in the low-energy theory [8, 11].

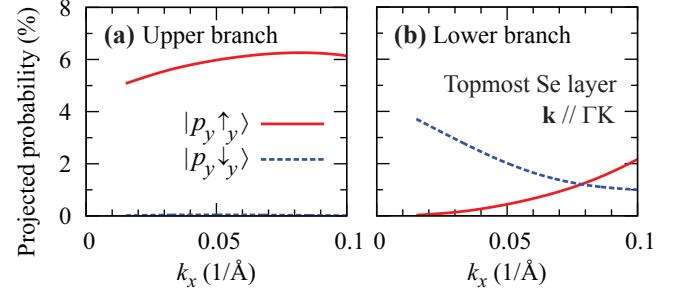


FIG. 6. Projected probability to the p_t orbital in the topmost atomic layer of the surface states with \mathbf{k} along ΓK as a function of k .

Figure 5 shows the extent of contribution of the p_t orbital (which is p_y) to the surface states in the lower branch with \mathbf{k} along ΓK , resolved to each spinor. Near Γ ($k = 0.015 \text{ \AA}^{-1}$), the p_y orbital in each layer couples exclusively to $|\downarrow_y\rangle$, as predicted by first-order $\mathbf{k} \cdot \mathbf{p}$ theory [11]. However, when $k = 0.106 \text{ \AA}^{-1}$, the coupling of p_y to $|\uparrow_y\rangle$ is significant and, especially, in the case of the topmost layer (which is the most important in photoemission processes), the projected probability to $|\uparrow_y\rangle$ is more than twice as high as that to $|\downarrow_y\rangle$.

Figure 6 shows the projected probability of the tangential p orbital at the topmost surface layer. For the surface state in the upper branch, the contribution from the term $|p_y \downarrow_y\rangle$, albeit not forbidden at large k , is negligible in the range of k considered. (In fact, this $|p_y \downarrow_y\rangle$ contribution is tiny up to the fourth atomic layers from the surface [14].) However, for the surface state in the lower branch at large k , the contribution of $|p_y \uparrow_y\rangle$ in the topmost layer outweighs that of $|p_y \downarrow_y\rangle$. (See Supplemental Material [14] for the layer-resolved projection to the three p orbitals.) This difference explains why, at large k , P_y of the photoelectrons from the upper branch excited by the s- and p-polarized lights have different signs [Fig. 4(a)], whereas P_y of the photoelectrons from the lower branch have the same sign [Fig. 4(b)].

In conclusion, we studied the possibility of modulating the electron spin through photoemission from the surfaces of Bi_2Se_3 and Au. We find that both (i) the intricate spin-orbital coupling and (ii) large- k effects are crucial in understanding and predicting the possibility of photo-induced spin modulation. Not only does our study provide an explanation of the recent low-energy, spin-dependent photoemission experiments in a coherent manner, it also establishes a designing principle for a new kind of spin-polarized electron sources using topological insulators.

We gratefully acknowledge fruitful discussions with X.J. Zhou on his experimental results in Ref. [10] and with Chris Jozwiak and Choongyu Hwang on many aspects of SARPES experiments on Bi_2Se_3 and Au (111). This work was supported by Korean NRF-

2013R1A1A1076141 funded by MSIP and computational resources were provided by Aspiring Researcher Program through Seoul National University in 2014.

- [18] H. Lee and H. J. Choi, Phys. Rev. B **86**, 045437 (2012).
 [19] H. Ishida, Phys. Rev. B **90**, 235422 (2014).

* cheolhwan@snu.ac.kr

- [1] M. Johnson and R. H. Silsbee, Phys. Rev. Lett. **55**, 1790 (1985).
 [2] D. T. Pierce and F. Meier, Phys. Rev. B **13**, 5484 (1976).
 [3] S. D. Sarma, J. Fabian, X. Hu, and I. Žutić, IEEE Trans. Magn. **36**, 2821 (2000).
 [4] T. Nakanishi, H. Aoyagi, H. Horinaka, Y. Kamiya, T. Kato, S. Nakamura, T. Saka, and M. Tsubata, Phys. Lett. A **158**, 345 (1991).
 [5] E. Bauer, T. Duden, and R. Zdyb, J. Phys. D: Appl. Phys. **35**, 2327 (2002).
 [6] R. Alley, H. Aoyagi, J. Clendenin, J. Frisch, C. Garden, E. Hoyt, R. Kirby, L. Klaisner, A. Kulikov, R. Miller, G. Mulhollan, C. Prescott, P. Sez, D. Schultz, H. Tang, J. Turner, K. Witte, M. Woods, A. Yeremian, and M. Zolotorev, Nucl. Instr. Meth. Phys. Res. A **365**, 1 (1995).
 [7] C. Jozwiak, C.-H. Park, K. Gotlieb, C. Hwang, D.-H. Lee, S. G. Louie, J. D. Denlinger, C. R. Rotundu, R. J. Birgeneau, Z. Hussain, and A. Lanzara, Nat. Phys. **9**, 293 (2013).
 [8] C.-H. Park and S. G. Louie, Phys. Rev. Lett. **109**, 097601 (2012).
 [9] C. Jozwiak, Y. L. Chen, A. V. Fedorov, J. G. Analytis, C. R. Rotundu, A. K. Schmid, J. D. Denlinger, Y.-D. Chuang, D.-H. Lee, I. R. Fisher, R. J. Birgeneau, Z.-X. Shen, Z. Hussain, and A. Lanzara, Phys. Rev. B **84**, 165113 (2011).
 [10] Z. Xie, S. He, C. Chen, Y. Feng, H. Yi, A. Liang, L. Zhao, D. Mou, J. He, Y. Peng, X. Liu, Y. Liu, G. Liu, X. Dong, L. Yu, J. Zhang, S. Zhang, Z. Wang, F. Zhang, F. Yang, Q. Peng, X. Wang, C. Chen, Z. Xu, and X. J. Zhou, Nat. Commun. **5**, 3382 (2014).
 [11] H. Zhang, C.-X. Liu, and S.-C. Zhang, Phys. Rev. Lett. **111**, 066801 (2013).
 [12] Z.-H. Zhu, C. Veenstra, G. Levy, A. Ubaldini, P. Syers, N. Butch, J. Paglione, M. Haverkort, I. Elfimov, and A. Damascelli, Phys. Rev. Lett. **110**, 216401 (2013).
 [13] Z.-H. Zhu, C. N. Veenstra, S. Zhdanovich, M. P. Schneider, T. Okuda, K. Miyamoto, S.-Y. Zhu, H. Namatame, M. Taniguchi, M. W. Haverkort, I. S. Elfimov, and A. Damascelli, Phys. Rev. Lett. **112**, 076802 (2014).
 [14] See Supplemental Material at <http://link.aps.org/xxx> for computational details and for a layer-resolved projection of the surface-state wavefunctions of Bi₂Se₃ to each p orbital.
 [15] Y. Cao, J. A. Waugh, N. C. Plumb, T. J. Reber, S. Parham, G. Landolt, Z. Xu, A. Yang, J. Schneeloch, G. Gu, J. H. Dil, and D. S. Dessau, arXiv:1211.5998v1.
 [16] J. Henk, A. Ernst, and P. Bruno, Phys. Rev. B **68**, 165416 (2003).
 [17] J. Sánchez-Barriga, A. Varykhalov, J. Braun, S.-Y. Xu, N. Alidoust, O. Kornilov, J. Minár, K. Hummer, G. Springholz, G. Bauer, R. Schumann, L. V. Yashina, H. Ebert, M. Z. Hasan, and O. Rader, Phys. Rev. X **4**, 011046 (2014).

Supplemental Material

CALCULATION DETAILS

We obtained the wavefunctions of surface states using Quantum Espresso package [S1]. We have modeled Bi₂Se₃ (111) and Au (111) surfaces by 30- and 24-atomic-layer slabs, respectively. We set the inter-slab distance to 20 Å for Bi₂Se₃ and 30 Å for Au. We fully relaxed the lattice parameters and the atomic positions taking into account, for Bi₂Se₃, van der Waals interactions. (We have checked that the relaxed structure of *bulk* Bi₂Se₃ is in very good agreement - less than 1 % differences in the lattice parameters and in the inter-quintuple-layer distance - with the measurement [S2].)

To describe ion-electron interactions, we used fully-relativistic, norm-conserving pseudopotentials. To account for exchange-correlation interactions, we used the method of Ref. [S3] for Bi₂Se₃ and that of Ref. [S4] for Au. The k-point meshes that we used for Bi₂Se₃ (111) and for Au (111) are $13 \times 13 \times 1$ and $12 \times 12 \times 1$, respectively. The kinetic energy cutoff is set to 60 Ry.

Photoexcited states are described, following Refs. [S5, S6], as the Bloch sum of *s*-like orbitals inside the crystal. A photoexcited state $|f\rangle$ can be approximated as, taking into account the phase of an electron emitted from each atom and inelastic collisions inside the crystal, $|f\rangle \approx |\psi\rangle \otimes |\chi\rangle$ with $\langle \mathbf{r} | \psi \rangle \propto \sum_{\mathbf{R}, \alpha} e^{z_\alpha/2\lambda} e^{i\mathbf{k}_f \cdot (\mathbf{R} + \boldsymbol{\tau}_\alpha)} \phi_\alpha(\mathbf{r} - \mathbf{R} - \boldsymbol{\tau}_\alpha)$ being the orbital part of the wavefunction and $|\chi\rangle$ the spin part (either spin-up or spin-down). Here, \mathbf{R} denotes the (in-plane) lattice vector, $\boldsymbol{\tau}_\alpha$ the position of an atom α within each unit cell of the slab, λ the inelastic mean free path of electrons, set to 7 Å [S5], and $\phi_\alpha(\mathbf{r} - \mathbf{R} - \boldsymbol{\tau}_\alpha)$ the orbital localized at each atomic site (see below for details).

The wavevector of a photoelectron $\mathbf{k}_f = (\mathbf{k}_{f,\parallel}, k_{f,z})$ and the wavevector of the initial surface electron \mathbf{k}_i are related by $\mathbf{k}_{f,\parallel} = \mathbf{k}_i$ and $k_{f,z} = \sqrt{2m(h\nu - E_B)/\hbar^2 - (k_{i,x})^2 - (k_{i,y})^2}$, where E_B is the binding energy of the surface state, m the mass of an

electron, and the photon energy, $h\nu$, is set to 6 eV [S5]. The calculations based on this scheme are proven to reproduce the measured spin polarization of photoelectrons from Bi₂Se₃ quite well [S6, S7].

We set $\phi_\alpha(\mathbf{r}) = c_\alpha e^{-r^2/R_0^2}$, where the parameter R_0 is set to be 0.3 times the lattice parameter, which is similar to the relevant atomic radii and c_α is an atomic-type-dependent constant. We checked that using the atomic valence *s* orbitals as $\phi(\mathbf{r})$'s yields essentially the same results. For the final states of Bi₂Se₃, we set c_α for Se to be twice as large as that for Bi in order to match the atomic cross sections of the two elements [S5].

* cheolhwan@snu.ac.kr

- [S1] P. Giannozzi, S. Baroni, N. Bonini, M. Calandra, R. Car, C. Cavazzoni, D. Ceresoli, G. L. Chiarotti, M. Cococcioni, I. Dabo, A. D. Corso, S. de Gironcoli, S. Fabris, G. Fratesi, R. Gebauer, U. Gerstmann, C. Gougoussis, A. Kokalj, M. Lazzeri, L. Martin-Samos, N. Marzari, F. Mauri, R. Mazzarello, S. Paolini, A. Pasquarello, L. Paulatto, C. Sbraccia, S. Scandolo, G. Sclauszero, A. P. Seitsonen, A. Smogunov, P. Umari, and R. M. Wentzcovitch, *J. Phys.: Condens. Matter* **21**, 395502 (2009).
- [S2] S. Nakajima, *J. Phys. Chem. Solids* **24**, 479 (1963).
- [S3] J. P. Perdew, K. Burke, and M. Ernzerhof, *Phys. Rev. Lett.* **77**, 3865 (1996).
- [S4] J. P. Perdew, A. Ruzsinszky, G. I. Csonka, O. A. Vydrov, G. E. Scuseria, L. A. Constantin, X. Zhou, and K. Burke, *Phys. Rev. Lett.* **100**, 136406 (2008).
- [S5] Z.-H. Zhu, C. Veenstra, G. Levy, A. Ubaldini, P. Syers, N. Butch, J. Paglione, M. Haverkort, I. Elfimov, and A. Damascelli, *Phys. Rev. Lett.* **110**, 216401 (2013).
- [S6] Z.-H. Zhu, C. N. Veenstra, S. Zhdanovich, M. P. Schneider, T. Okuda, K. Miyamoto, S.-Y. Zhu, H. Namatame, M. Taniguchi, M. W. Haverkort, I. S. Elfimov, and A. Damascelli, *Phys. Rev. Lett.* **112**, 076802 (2014).
- [S7] J. Sánchez-Barriga, A. Varykhalov, J. Braun, S.-Y. Xu, N. Alidoust, O. Kornilov, J. Minár, K. Hummer, G. Springholz, G. Bauer, R. Schumann, L. V. Yashina, H. Ebert, M. Z. Hasan, and O. Rader, *Phys. Rev. X* **4**, 011046 (2014).

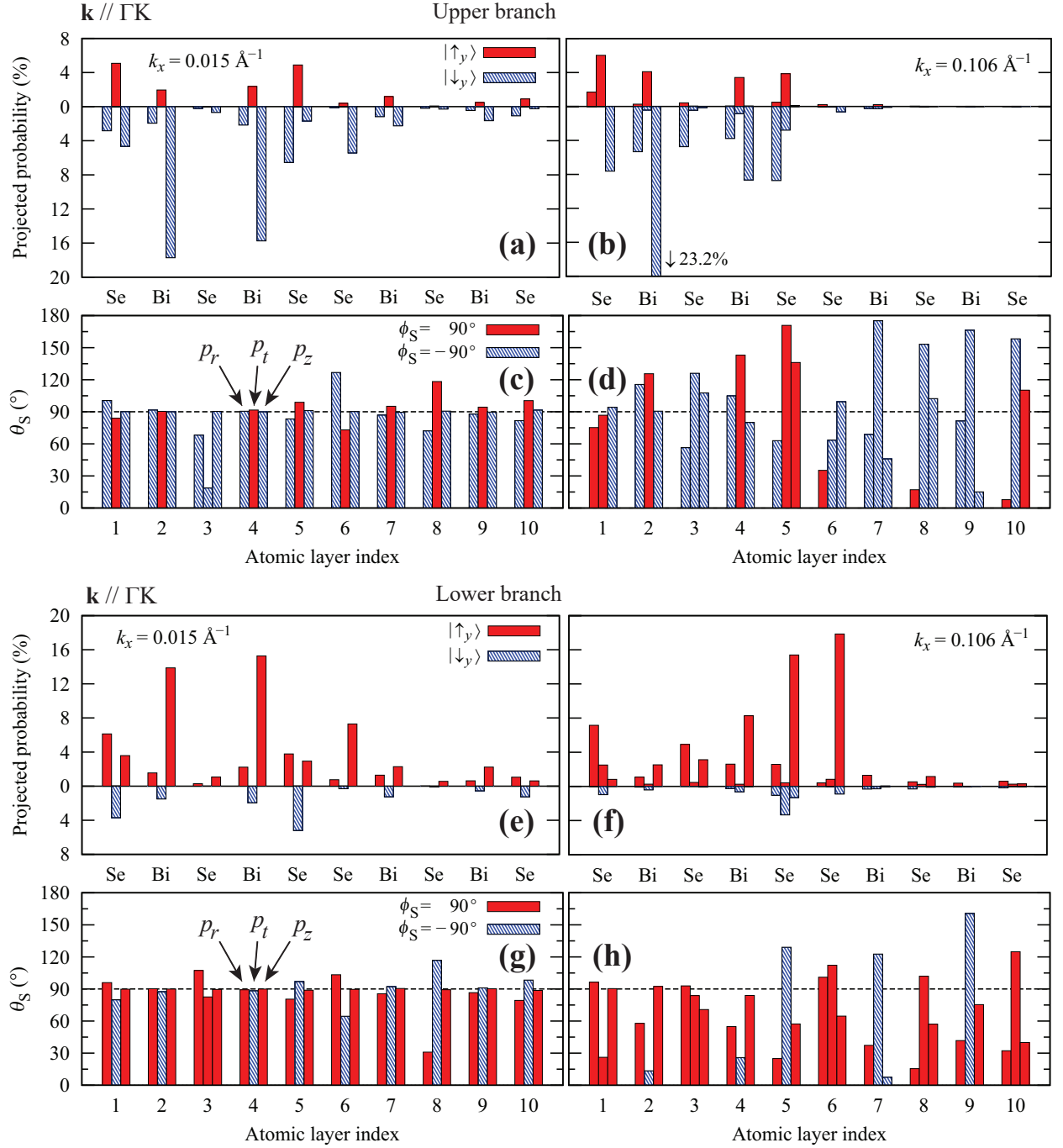


FIG. S1. (a) and (b) Projected probability of the surface states in the upper branch with \mathbf{k} along ΓK and at $k = 0.015 \text{ \AA}^{-1}$ [(a)] and at $k = 0.106 \text{ \AA}^{-1}$ [(b)]. The spin is quantized along y [the tangential direction; see Fig. 1(a) of the main manuscript]. Atomic layer 1 is the topmost surface layer. (c) and (d) The direction of the spin polarization corresponding to a spinor that couples to each p orbital, for the same surface states as in (a) and (b), respectively. Spin direction ($\sin \theta_S \cos \phi_S$, $\sin \theta_S \sin \phi_S$, $\cos \theta_S$) is represented by the two angles θ_S and ϕ_S . (e)-(h) Similar quantities as in (a)-(d) for the lower branch.